Abstract

GARNER, JOHN DAIL. Numerical and Experimental Investigation of Biodiesel/Glycerin Separation. (Under the direction of Alexander O. Hobbs.)

During the production of biodiesel, oils and fats are vigorously mixed with an alcohol to produce biodiesel and glycerin. These two fluids need to be separated in order to obtain a pure stream of biodiesel. In continuous flow biodiesel production facilities, centrifuges are used to aid in this separation; however, centrifuges are expensive to purchase and operate, especially for small scale producers. For this reason, an alternative to centrifuges is needed for continuous production by small scale producers.

In this biodiesel/glycerin mixture, small droplets of glycerin are dispersed within the biodiesel. If this mixture is placed into a tank where fluid motion is absent, gravity causes the droplets to settle out and form a layer of glycerin below the biodiesel. After the separation has occurred, the glycerin and biodiesel can be drained off separately. This is the technique that batch production facilities use. Using this technique, it is possible to use a series of tanks as a continuous flow separation device. While one tank was being filled, others would be settling. Once settled, the phases could be drained off and the tanks could be refilled.

In order to predict whether the separation times are acceptable for biodiesel producers, a simple model is needed. In 1997, Parichay K. Das proposed such a model in his paper entitled “Prediction of Settling Velocities of Drops in a Concentrated Batch Liquid-Liquid Dispersion.” In the present work, the estimated separation times from this model are compared to experimentally determined settling times. It was hoped that this model could accurately predict the separation time for this liquid-liquid dispersion; however, after comparison, it was determined that the model didn’t accurately predict these settling times.

Possible sources of error are discussed; however, no one reason for the model discrepancy could be determined.

In the present work, a continuous separation process was designed to mate onto a continuous flow production facility that was developed by researcher at the University of Idaho. A simple bank of 5 small tanks was designed to replace the centrifuge that the Idaho researcher proposed. This design was based on Das's model, even though the model was suspected of overestimating the settling times.

NUMERICAL AND EXPERIMENTAL INVESTIGATION OF BIODIESEL/GLYCERIN SEPARATION

by
JOHN DAIL GARNER

A thesis submitted to the Graduate Faculty of
North Carolina State University
in partial fulfillment of the
requirements for the Degree of
Masters of Science

MECHANICAL AND AEROSPACE ENGINEERING

Raleigh

2005

APPROVED BY:

Chair of Advisory Committee

Personal Biography

John Dail Garner born and raised in Kenansville, NC. He earned his Bachelors of Science degree in mechanical engineering from NC State University in 2003. Immediately upon completion of that degree, he returned to NC State to pursue his Masters of Science in Mechanical Engineering. During the final year of his undergraduate degree, John considered energy conservation, energy efficiency, and renewable energy as possible research projects. While pursing his Masters, John worked for the North Carolina Solar Center. It was this job that gave John the opportunity to be involved with all forms of renewable energy projects, including wind turbines, anaerobic digestion, biomass, combined heat and power, and biodiesel.

Table of Contents

List of Figures

List of Tables

List of Symbols

Letters:

A	Area [m^2]
B	Buoyancy force [N]
C_D	Drag coefficient [-]
D	Droplet diameter [m]
d	Distance [m]
d_c	Settling column diameter [m]
E	Energy [J]
f	Flux of droplets [$1/m^2s$]
F_D	Drag force [N]
$\tilde{f}$	Dimensionless flux of drops [-]
g	Function label [-]
$\tilde{g}$	Dimensionless function label [-]
I_W	Immersed Weight [N]
L	Settling column length [m]
m_d	Displaced mass [kg]
n	Number density [$1/m^3$]
$n_{\max}$	Maximum number density [$1/m^3$]
Re	Reynolds number [-]
s	Coalescing parameter [-]
S_t	Separation front velocity [m/s]

t	Time [s]
t_s	Settling time [s]
$\tilde{t}$	Dimensionless time [-]
$\tilde{t}_s$	Dimensionless settling time [-]
u	Settling velocity [m/s]
$u_{\max}$	Maximum settling velocity [m/s]
V	Volume of droplet [m^3]
V_d	Displaced volume [m^3]
$V_{continuous}$	Continuous phase volume [m^3]
$V_{dispersed}$	Dispersed phase volume [m^3]
W	Weight [N]
x	Distance [m]
$\tilde{x}$	Dimensionless distance [m]

Greek:

ε	Dispersed phase volume fraction [-]
ε_0	Initial dispersed phase volume fraction [-]
ρ_c	Density of continuous phase [kg/m^3]
ρ_d	Density of dispersed phase [kg/m^3]
μ_c	Viscosity of continuous phase [kg/m^3]
μ_d	Viscosity of dispersed phase [kg/m^3]

1.1 Oil Consumption vs. Production

The United States of America currently consumes 26% of the world's oil production. By far, the US uses the greatest percentage of the world's oil, with the next 6 countries, including Japan, China, Germany, Russia, Brazil, and South Korea, consuming only 25.5% of the oil produced.

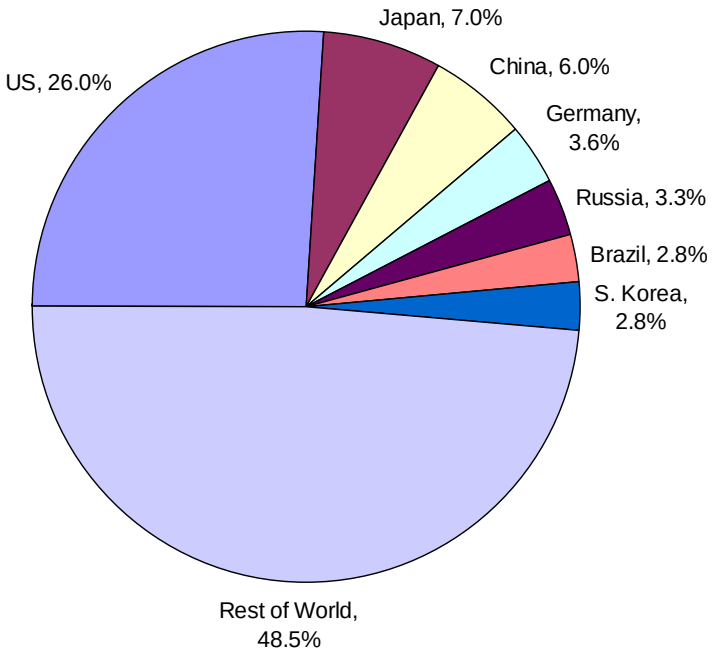

Figure 1.1.1: Breakdown of world oil consumption (Frontline 2002)

With its insatiable appetite for oil, the US has been relying on imported oil more heavily ever since US oil production peaked in the 1970's. US oil production is currently just under 8.2 million barrels per day, while it currently consumes close to 20 million barrels of oil per day. This results in the US importing 58% of the oil it consumes (Frontline 2002). It has been estimated that within the next ten years, 70% of the oil consumed in the US will need to be imported (NBB 2004).

1.2 Diesel Consumption

US diesel fuel consumption for transportation use has been holding steady for the past five years. Usage has remained constant at just under 140 million gallons per day. In 1999, of all the petroleum used in the US, 12% was used to create on-road diesel fuel; however, it is estimated that approximately 9% of this on-road diesel was used for home heating and off-road applications (EIA 2005).

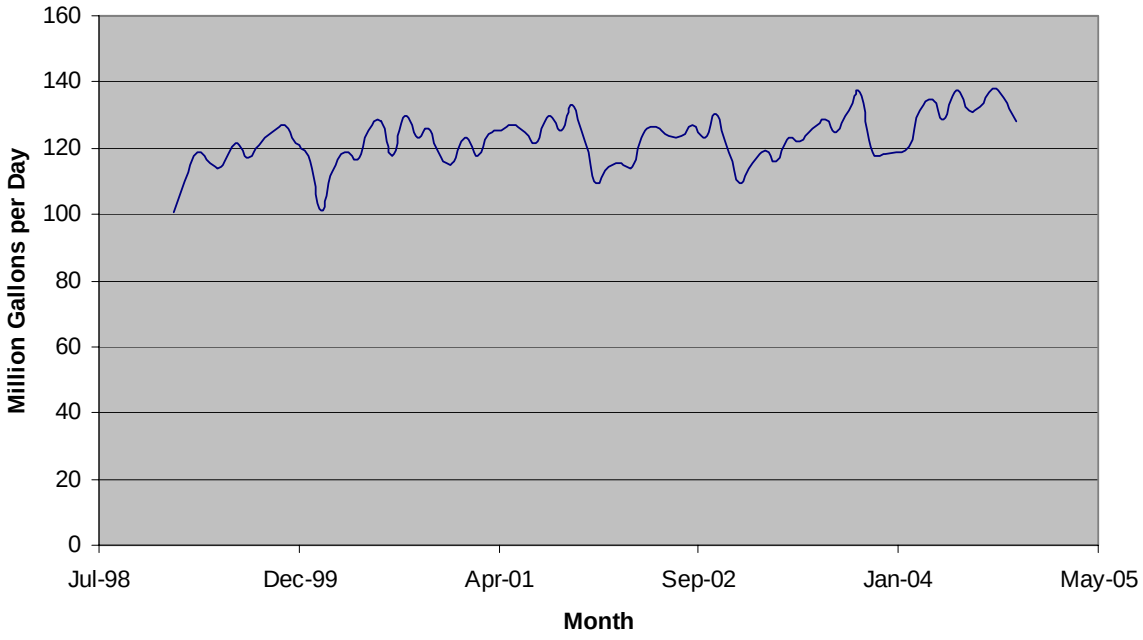

Figure 1.2.1: Daily usage of diesel fuel for transportation (EIA 2005)

1.3 Alternatives Fuels

One widely accepted alternative to conventional diesel fuel is biodiesel. Biodiesel can be produced through several chemical processes, which produce alkyl monoesters, the chemical name for biodiesel (NBB 2004). Biodiesel can be produced from vegetable oils and animal fats. The recent decline in US oil production and a renewed interest in the environment caused many people to reevaluate the possibility of using renewable fuels

instead of fossil fuels (Pahl 2005). For all these reasons, biodiesel has become a popular alternative to conventional petroleum diesel.

Using fats and oils as fuel is not a new idea. Rudolf Diesel, the inventor of the diesel engine, was a strong advocate for the use of these products. At the Paris Exhibition of 1900, Diesel showcased one of his engine's running on peanut oil. Later, in a 1912 speech, he said "the use of vegetable oils for engine fuels may seem insignificant today, but such oils may become, in the course of time, as important as petroleum." He went on to say that "power can still be produced from the heat of the sun, always available, even when the natural stores of solid and liquid fuels are completely exhausted." Up until his death in 1913, Diesel continued to advocate the use of vegetable oils as a fuel for his new engine (Pahl 2005).

In October of 2004, over twenty companies in the US were producing biodiesel. It is estimated that these plants could produce as much as 150 million gallons of biodiesel per year. However, it has been estimated that domestic production of biodiesel could easily be doubled or tripled within 12 months (NBB 2004). Using the conservative estimate of a two-fold increase in production, the US could offset 300 million gallons of on-road diesel fuel with domestically produced biodiesel every year. This equates to about one day's worth of diesel fuel consumption.

There are many advantages to biodiesel versus conventional petroleum diesel. Biodiesel can be used in any diesel engine, usually with no modifications, and results in no significant power loss or fuel efficiency reductions. Significant emissions reductions are realized by using biodiesel as well. Another significant difference between biodiesel and diesel is the energy required to produce both. In the production process of biodiesel, for every 3.2 units of energy produced as fuels, only 1 energy unit is consumed. This is a much

more favorable energy balance than the 1.2 units needed to produce 1 unit of petroleum diesel. Biodiesel boosts the highest such energy balance of any current fuel. Another major advantage is the low toxicity levels of biodiesel, with a lethal dose of 17.4 g/kg of body weight. By comparison, this is nearly an order of magnitude larger than the lethal dose of table salt. However, the most important benefit of biodiesel is economic. It has been estimated that for every billion dollars spent on oil imports, the US looses as many as 25,000 jobs (NBB 2004).

2 Biodiesel Production

2.1 Overview

There are three basic methods to produce biodiesel from animal fats and vegetable oils. These methods are (NBB 2004):

- "Base catalyzed transesterification of the oil with alcohol"
- "Direct acid catalyzed esterification of the oil with methanol"
- "Conversion of the oil to a fatty acid, and then to alkyl esters with acid catalyst"

The first method, base catalyzed transesterification, is currently the most preferred method of biodiesel production. The six main reasons for this preference are (NBB 2004):

- Relatively low temperatures, usually under 150° F
- Relatively low pressures, usually under 20 psi
- Very high conversion rates, in excess of 97%
- Minimal side reactions, which allows for very fast reaction times
- Direct formation of monoesters without intermediate steps
- No need for unusual materials or construction practices

The basic reaction involves an oil molecule reacting with an alcohol in the presence of a catalyst. The three fatty acid chains of the triglyceride are broken off of the glycerol backbone. The alcohol lends its hydrocarbon chain to the ester, while its OH group goes into the formation of the glyceride molecule.

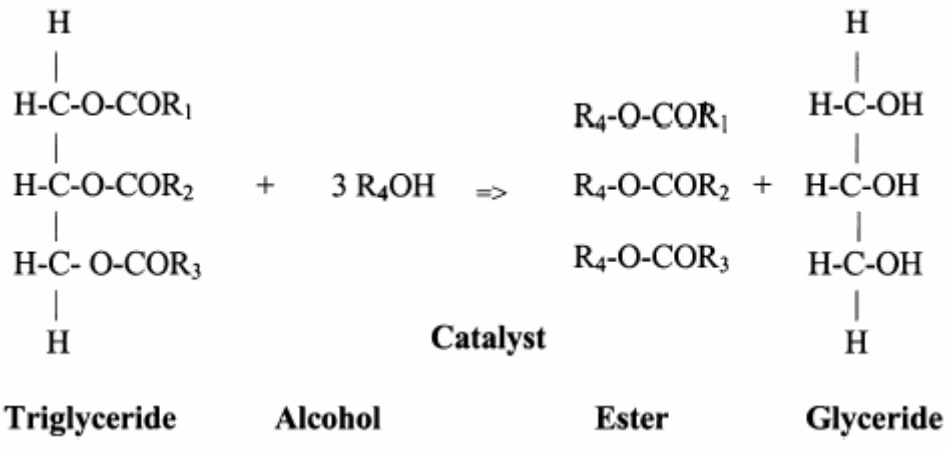

Figure 2.1.1: Transesterification reaction (Peterson et al 2002)

The basic steps in producing biodiesel through base catalyzed transesterification are described below; however, a more detailed explanation will be presented in Chapter 3.

An alcohol, usually methanol, is mixed with a base catalyst, such as NaOH or KOH. The amount of catalyst and alcohol are determined from the quantity and quality of the feedstock used. Next, these two substances are introduced into a reaction vessel were they are thoroughly mixed, at which point the reaction in Figure 2.1.1 takes place. Once this reaction has completed, the resulting biodiesel/glycerin mixture is separated. Then additional processes are performed to remove any excess catalyst or alcohol and to purify the biodiesel and glycerin to prepare the products for sale.

There are two different biodiesel production techniques, batch and continuous processes, that can employ the base catalyzed transesterification process. In a batch process, the reaction and settling occur via gravity, usually in the same vessel or tank. However, in a continuous process, feedstock, alcohol, and catalyst are constantly being added to and biodiesel and glycerin are constantly being removed from the process.

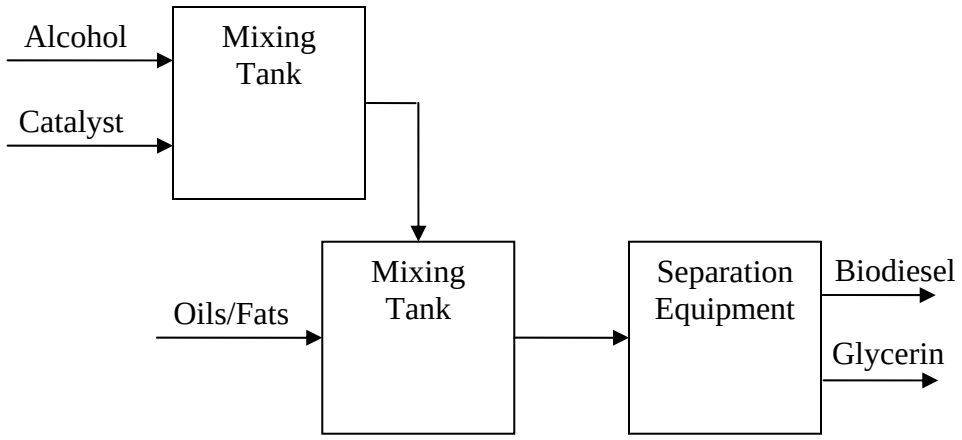

Figure 2.1.2: Process flow diagram (PFD) of biodiesel via transesterification

2.2 Separation Options

There are two separation options that can be used in biodiesel production, gravity and centrifuges. In gravity separation, tanks are filled with a biodiesel/glycerin mixture and allowed to separate. This process is fairly inexpensive; however, the trade off is that the process is relatively time intensive. In centrifugal separation, centrifuges are fed a biodiesel/glycerin mixture and the high acceleration forces quickly separate the mixture. Centrifuges are expensive to purchase and operate due to the substantial amounts of power consumed.

The decision of which separation process to use is usually determined by the process chosen. For batch processes, gravity separation is usually used, and for continuous processes, centrifuges are the current option of choice. However, some researchers have posed the possibility of using centrifuges in batch operation to increase the throughput of the plant (C. Thrasher, personal communication, Mar. 15, 2005).

3 Gravity Separation

3.1 Introduction

Liquid-liquid dispersions are very common in many industrial processes. There are several options that can be used to separate these phases. As mentioned earlier, centrifuges can be used to separate the dispersion. Parallel plate coalescers can also be used, and so can filters and special membranes. The easiest and perhaps the most inexpensive method is gravity separation. The density difference between the fluids is the basis for gravity separation. For two phase liquid-liquid dispersions, the liquid with the largest volume is referred to as the continuous phase, while the liquid of least volume is referred to as the dispersed phase. For the purposes of this discussion, it is assumed that the dispersed phase (glycerin) has a higher density than that of the continuous phase (biodiesel). For gravity separation of these two phase dispersions, there are two typical characteristics that can be observed, sedimentation and coalescence (Nadiv and Semiat 1995).

Coalescence occurs when a front develops between the pure continuous phase and the mixed continuous and dispersed phases. This usually occurs because there are a large number of dispersed phase droplets falling through the liquid-liquid dispersion. When the population of these droplets is high enough, individual droplets begin to interact with each other while falling. A coalescing front forms as these droplets interact with each other. The droplets usually merge with one another until they are large enough to break free of the front and continue settling to the bottom of the column. This front moves downward with time as the dispersed phase droplets continue to coalesce and settle.

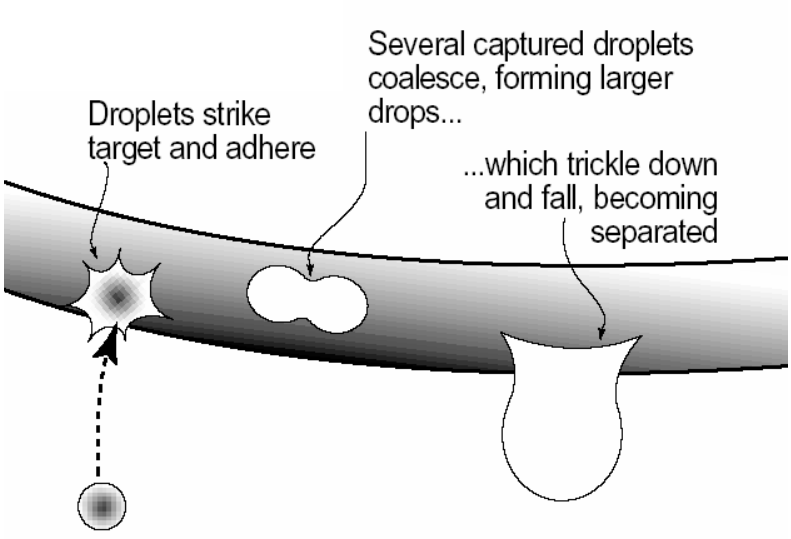

Figure 3.1.1: Diagram of coalescence (ACS 2003)

As droplets of the dispersed phase fall, they begin to form a large mass at the bottom of the settling column. The sedimentation front separates the pure dispersed phase and the mixed region of the dispersed and continuous phases. The droplets that reach the sedimentation front can be generated in two ways. The drops can be created by the coalescence front, as described earlier, or they can simply be droplets of the dispersed phase that occur without coalescing.

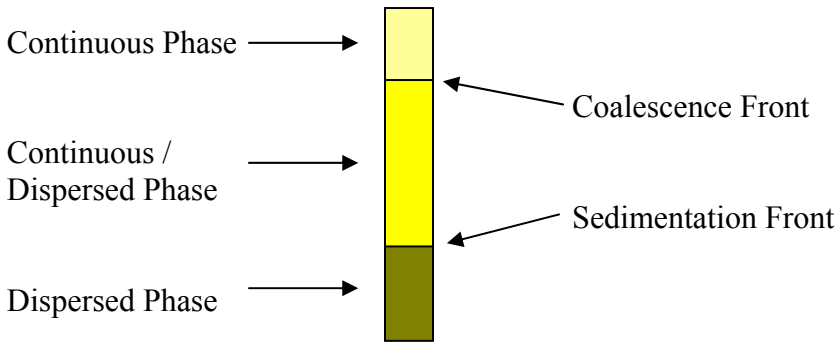

Figure 3.1.2: Representation of settling fronts

In liquid-liquid dispersions that are not emulsions, sedimentation usually occurs; however, coalescence may not always occur. This is the case for the biodiesel/glycerin

mixture. A coalescence front never forms, but the sedimentation front forms at the bottom of the settling column and moves upward until all the glycerin is removed from the biodiesel.

3.2 Numerical Model

Many numerical models exist that can be used to predict the separation time of liquid-liquid dispersions. For the purpose of this research, a simple model was needed in order to be easily deployed in real-world biodiesel production facilities. Such facilities have limited knowledge of liquid-liquid dispersions; therefore, a simple model is a must. After an extensive literature search, a model that was proposed by Das in 1997 was determined to be appropriate for the needs described above. The following discussion lays out the development of Das's model. The basis for a majority of this discussion was extracted for Das's work (1997).

The general continuity equation for liquid-liquid dispersions in a constant cross-sectional area column, with uniformly distributed droplets of the dispersed phase is

$$\frac{\partial n}{\partial t} + \frac{\partial f}{\partial x} = s \qquad (3.2.1)$$

Where n represents the number density, or the droplets per unit area, and f represents the flux of the dispersed phase droplets. When u is the velocity of a droplet, $f = u \cdot n$. When coalescence is involved, s is a parameter to account for the collection of droplets into larger droplets. Coalescence doesn't appear to occur in the biodiesel/glycerin separation; therefore, for the biodiesel/glycerin mixture $s = 0$; therefore,

$$\frac{\partial n}{\partial t} + \frac{\partial f}{\partial x} = 0 \qquad (3.2.2)$$

Consider a control volume of biodiesel that contains N droplets of a glycerin dispersed within it. It is evident that this equation holds true since the number of droplets within the control

volume will only change if there is a net change in the flux of droplets across the control volume boundary. For instance, if 5N droplets enter and 3N droplets leave the control volume due to flux, then 2N have stayed in the control volume; therefore, the number of droplets has increased by 2N.

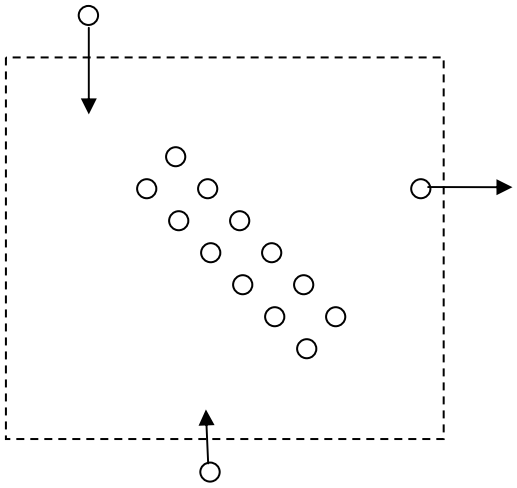

Figure 3.2.1: Control volume of liquid-liquid dispersion

The continuity equation can be re-written as

$$\frac{\partial n}{\partial t} + \frac{df}{dn} \cdot \frac{\partial n}{\partial x} = 0 \tag{3.2.3}$$

Let u represent the settling velocity of a dispersed phase droplet and define it as

$$u(n) = u_{\max} g(n) \tag{3.2.4}$$

where g is a generic monotonically decreasing function of n that is dimensionless. Now assume that

$$\lim_{n \to 0} g(n) = 1 \tag{3.2.5}$$

and

$$\lim_{n \to n_{\max}} g(n) = 0 \tag{3.2.6}$$

Following these assumptions, $u(n) = u_{\max}$ when the number density of the dispersed phase droplets is very small. Intuitively, this is known to be true, for when a single dispersed phase droplet falls through the continuous phase with no interaction of other droplets, the droplet will fall at its maximum possible velocity. However, when the population of these droplets is high, $u(n) = 0$. This also makes sense when the sedimentation front is examined. As a droplet approaches this front, its velocity slows and reaches zero as it reaches the front, which represents an area of high dispersed phase droplet population. When $n = 0$ or $n = n_{\max}$, it is known that $f(n) = 0$ due to the fact that there are no concentration gradients left to drive the flux.

There is an inherent problem with characterizing the settling velocity as a function of the droplet number density. This property is difficult and expensive to measure; therefore, a more readily available measurement must be used to correlate this velocity. One such parameter that is easy to measure is the initial dispersed phase volume fraction, which can be defined as

$$\varepsilon_0 = \frac{V_{Dispersed}}{V_{Dispersed} + V_{Continuous}} \tag{3.2.7}$$

At this point, the introduction of two more dimensionless variables for time and distance will make further derivation easier. Dimensionless time is defined as

$$\tilde{t} = \frac{u_{\max} t}{L} \tag{3.2.8}$$

and dimensionless distance is defined as

$$\tilde{x} = \frac{x}{L} \tag{3.2.9}$$

where x is the distance from the top of the settling column measuring toward the bottom and L is the total height of the settling column.

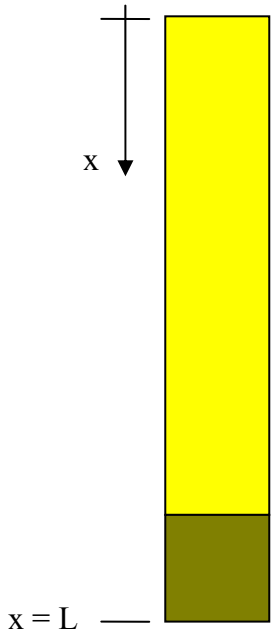

Figure 3.2.2: Schematic of x and L

Define a dimensionless function for the flux as

$$\widetilde{f}(\varepsilon) = \frac{f(n)}{u_{\max} n_{\max}} \tag{3.2.10}$$

Recall that $g(n)$ was defined arbitrarily in (3.2.4), now redefine this function as

$$\widetilde{g}(\varepsilon) = g(n) \tag{3.2.11}$$

Recall the base conservation equation, (3.2.3)

$$\frac{\partial n}{\partial t} + \frac{df}{dn} \cdot \frac{\partial n}{\partial x} = 0 \tag{3.2.12}$$

Replacing n and f by their dimensionless equivalents of ε and $\widetilde{f}$ respectively yields

$$\frac{\partial \varepsilon}{\partial t} + \frac{d\widetilde{f}}{d\varepsilon} \cdot \frac{\partial \varepsilon}{\partial x} = 0 \tag{3.2.13}$$

The initial condition for this equation is

$$\varepsilon = \varepsilon_0 \text{ when } \tilde{t} = 0 \tag{3.2.14}$$

and the boundary condition is

$$\varepsilon = 0 \text{ when } \tilde{x} = 0 \tag{3.2.15}$$

Although no coalescence occurs and was not seen in experimentation, theoretically there is a separation front, above which only continuous phase liquid exists. The liquid below this front is a mixture of the dispersed and continuous phases until this separation front meets the sedimentation front. The settling rate, or velocity, of this separation front can be described as

$$S_t = \frac{d\tilde{x}}{d\tilde{t}} \tag{3.2.16}$$

This velocity is dependent upon the relationship of ε and $\tilde{f}$ in the following manner

$$\frac{d\tilde{x}}{d\tilde{t}} = \frac{\tilde{f}(0) - \tilde{f}(\varepsilon_0)}{0 - \varepsilon_0} \tag{3.2.17}$$

Recall that $f(0) = 0$, which leads to $\tilde{f}(0) = 0$; therefore, the separation front velocity reduces to

$$\frac{d\tilde{x}}{d\tilde{t}} = \frac{\tilde{f}(\varepsilon_0)}{\varepsilon_0} \tag{3.2.18}$$

Recall the initial conditions for the continuity equation deal with $\tilde{x} = 0$; therefore, the separation front velocity is a constant that depends upon ε only. Since $\tilde{g}$ was picked arbitrarily in (3.2.4) and (3.2.11) and ε_0 is a constant, let

$$\frac{d\tilde{x}}{d\tilde{t}} = \tilde{g}(\varepsilon_0) \tag{3.2.19}$$

Integration of this term yields

$$\tilde{t}_s = \frac{1-\varepsilon_0}{\tilde{g}(\varepsilon_0)} \tag{3.2.20}$$

where $\tilde{t}_s$ is the dimensionless time required for complete separation of the liquid-liquid dispersion. Combining this equation and the definition for $\tilde{t}_s$ results in

$$\frac{u_{\max} t_s}{L} = \frac{1-\varepsilon_0}{\tilde{g}(\varepsilon_0)} \tag{3.2.21}$$

where t_s is the dimensionless time required for complete separation. Further discussion about the choice of $\tilde{g}(\varepsilon_0)$ will follow the experimental results given in the next section. Other than $\tilde{g}(\varepsilon_0)$, all quantities are known in this equation, with the exception of $u_{\max}$. Das suggests using the velocity as defined by Stokes' Law.

3.3 Stokes' Law

The following discussion lays out the derivation of the Stokes' Velocity. The basis for a majority of this work was extracted from the work of White (2003).

Consider a spherical dispersed phase droplet falling through the motionless continuous phase. Initially, the dispersed phased droplet has a velocity of zero; however, the droplet accelerates as it falls until it reaches its terminal velocity. The terminal velocity occurs when the drag force, F_d, is balanced by the immersed weight, I_W, of the droplet. This can be written as

$$F_d = I_W \tag{3.3.1}$$

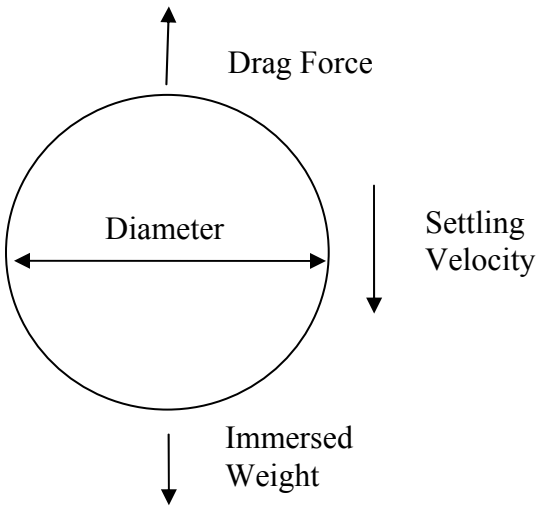

Figure 3.3.1: Spherical droplet

As the droplet falls through the continuous phase, it displaces a volume of the dispersed phase fluid. The kinetic energy required to accomplish this is defined as

$$E = \frac{1}{2} m_d u^2 \tag{3.3.2}$$

Where E is energy, m_d is the displaced mass, and u is the settling velocity. The cross-sectional area, A, of the spherical droplet is known to be

$$A = \frac{\pi D^2}{4} \tag{3.3.3}$$

where D is the diameter of the droplet. As the droplet falls through the continuous phase, over some distance d, the volume of liquid displaced, V_d, is known to be

$$V_d = \frac{d\pi D^2}{4} \tag{3.3.4}$$

Multiplying this equation by the density of the continuous phase liquid, ρ_c, yields the mass of fluid that is displaced by the droplet over distance d as

$$m_d = \frac{\rho_c d \pi D^2}{4} \tag{3.3.5}$$

Combining this equation with the definition for the kinetic energy required of the droplet yields

$$E = \frac{1}{2}\frac{\rho_c d \pi D^2}{4} u^2 \tag{3.3.6}$$

Since energy is defined as a force applied over a distance, this equation can be rewritten as

$$F_D d = \frac{1}{2}\frac{\rho_c d \pi D^2}{4} u^2 \tag{3.3.7}$$

where F_D is defined as the drag force. Rearrange to yield

$$F_D = \frac{\rho_c u^2 \pi D^2}{8} \tag{3.3.8}$$

This equation defines the theoretical drag force of a fully immersed sphere that is falling through a fluid. In order to account for fluid viscosity and dynamics of flow, the drag coefficient, C_D , is introduced as

$$F_D = C_D \frac{\rho_c u^2 \pi D^2}{8} \tag{3.3.9}$$

In order to characterize the flow of the continuous fluid around the droplets, the Reynolds number is introduced as

$$\mathrm{Re} = \frac{u \rho_c D}{\mu_c} \tag{3.3.10}$$

where μ_c is the continuous phase viscosity. Assuming that the Reynolds number is much less than 1, Stokes provides the drag force of a sphere as

$$F_D = 3 \pi D u \mu_c \tag{3.3.11}$$

Recall that the immersed weight is balanced by the drag force of the droplet. The immersed weight of the droplet is defined as

$$I_W = W - B \tag{3.3.12}$$

where W is the weight of the droplet and B is the buoyant force that the continuous phase fluid imparts on the droplet. W is defined as

$$W = V \cdot \rho_d \cdot g \tag{3.3.13}$$

where V is the volume of the droplet, ρ_d is the density of the dispersed phase liquid, and g is acceleration due to gravity. Define the volume of a sphere as

$$V = \frac{1}{6}\pi D^3 \tag{3.3.14}$$

Therefore,

$$W = \frac{1}{6}\pi D^3 \rho_d g \tag{3.3.15}$$

The buoyant force B that the droplet experiences is equal to the weight of the continuous phase liquid that the droplet displaces. This can be defined as

$$B = \frac{1}{6}\pi D^3 \rho_c g \tag{3.3.16}$$

Combining (3.3.15) and (3.3.16) along with (3.3.12) yields

$$I_W = \frac{1}{6}\pi D^3 \rho_d g - \frac{1}{6}\pi D^3 \rho_c g \tag{3.3.17}$$

Simplifying yields

$$I_W = \frac{1}{6}\pi D^3 g(\rho_d - \rho_c) \tag{3.3.18}$$

Remaining with the assumption that $\mathrm{Re} << 1$, (3.3.1) and (3.3.11) can be substituted into (3.3.18) to produce

$$3\pi Du\mu_c = \frac{1}{6}\pi D^3 g(\rho_d - \rho_c) \tag{3.3.19}$$

Rearranging and solving for the settling velocity gives

$$u = \frac{D^2 g(\rho_d - \rho_c)}{18\mu_c} \tag{3.3.20}$$

This equation is more commonly known as Stokes' Law or the Stokes' Velocity, so named after the British physicist G. G. Stokes. Combining the relationship developed in the previous sections, (3.2.21), and the above equation, (3.3.20), results in Das's model being defined as

$$\frac{D^2 g(\rho_d - \rho_c)t_s}{18\mu_c L} = \frac{1-\varepsilon_0}{\tilde{g}(\varepsilon_0)} \tag{3.3.21}$$

As stated earlier, there are several choices that have been presented for $\tilde{g}(\varepsilon_0)$ in the literature. Once the experimental data is presented, the appropriate choice will be made.

3.4 Experimental Setup

In order to determine if Das's separation model could be applied to the biodiesel/glycerin mixture, experiments were conducted to determine the nature of this separation process and the amount of time that is needed to allow for complete separation of the mixture.

In Das's model, the only parameter that the researcher has control over is the length of the settling column L. Das made no mention of any constraints on L during the derivation of his model. Another parameter which doesn't show up in the model, that the researcher can

control, is the diameter of the settling column d_c. Navid and Semiat used settling columns with diameters of 2.3 cm and 6.3 cm for similar settling experiments (1995). Two different diameters were chosen for this experimentation, one within the range suggested by Navid and Semiat and one even larger. The larger diameter was chosen to ensure that wall effects were negligible during testing. Another parameter that could be controlled is the initial dispersed phase volume fraction, ε_0; however, all the biodiesel used during this experimentation was produced from a consistent recipe; therefore, ε_0 is constant.

The experimentation included four test setups, with twenty tests for each test setup. Each setup consisted of a different combination of settling column diameter and height.

Table 3.4.1: Description of test setups

Test Setup #	Column Diameter (cm)	Length of Settler (cm)
I	4.8	13.1
II	4.8	25.2
III	8.0	13.1
IV	8.0	25.2

Four batches of biodiesel and glycerin were produced for use in these experiments. The following is a detailed description of the process that was used to produce a sample through transesterification.

1) 83 ml of 99.9% pure methanol was added to 2.3 g of KOH
2) This mixture was mixed until all the KOH was dissolved into the alcohol
3) This mixture was then added to 415 ml of Whole Harvest SmartFry® soybean oil

4) The combined mixture of oil, alcohol and catalyst was mixed for approximately 15 minutes at a high mixing intensity
5) The sample was allowed to react undisturbed for 24 hours
6) After 24 hours, the sample was remixed for 15 minutes
7) Steps 5 and 6 were repeated two more time to further ensure that the sample was fully reacted
8) During the duration of these steps and the experimentation, the sample remained sealed in an airtight container to avoid contamination

This process was repeated three more time to produce a total of 4 samples, lettered A through D. Sample D was treated as a control. It was not used in experimentation, but rather as a baseline reference for the density and viscosity of the biodiesel and glycerin. The other three samples, A through C, were used in the four test setups.

The following description is for a test that was conducted using test setup III. A similar process was used for all other tests.

1) A clear graduated cylinder that has measured diameter of 8 cm was chosen
2) The settling column height of 13.1 cm was marked on the side of the column
3) Samples B and C were combined in a 1000 ml Pyrex® bottle
4) The samples were mixed vigorously in the bottle
5) The mixture was poured into the settling column until the liquid level matched the predetermined column height of 13.1 cm

6) Inspecting the color of the liquid-liquid dispersion ensured an even distribution of droplets, if discolorations were seen, the mixture was returned to the bottle and the procedure returned to Step 4
7) Any excess liquid remained in the airtight bottle
8) The top of the settling column was plugged with a standard rubber laboratory stopper to ensure the test sample wasn't contaminated
9) The first test in a new test setup was allowed to settle for 24 hours to ensure all glycerin had settled from the biodiesel
10) After 24 hours, the position of the sedimentation front was noted
11) The test sample was then poured back into the airtight bottle
12) The biodiesel/glycerin mixture was well agitated
13) The mixture was then poured back into the column, up to a height of 13.1 cm
14) As soon as the liquid-liquid dispersion was added to the column, a stopwatch was started
15) Inspecting the color of the liquid-liquid dispersion ensures a uniform distribution of droplets, if discolorations were seen, the mixture was returned to the bottle and the procedure returned to Step 11
16) As the sedimentation front moved upward from the bottom of the column, its position was compared to the height measured in Step 10
17) Once the sedimentation front reached its final position, the time was noted

18) Steps 11 through 17 were repeated until 20 tests had been performed, resulting in 20 data points

19) At the conclusion of each set of test, the volume of glycerin and biodiesel was measured

A small wattage incandescent bulb was place behind the graduated cylinder in order to shine light through the liquid-liquid dispersion. This enables the sedimentation front to be seen easily. Figures 3.4.1a through 3.4.1.f are a set of pictures of a test in progress that were taken at intervals of approximately one minute.

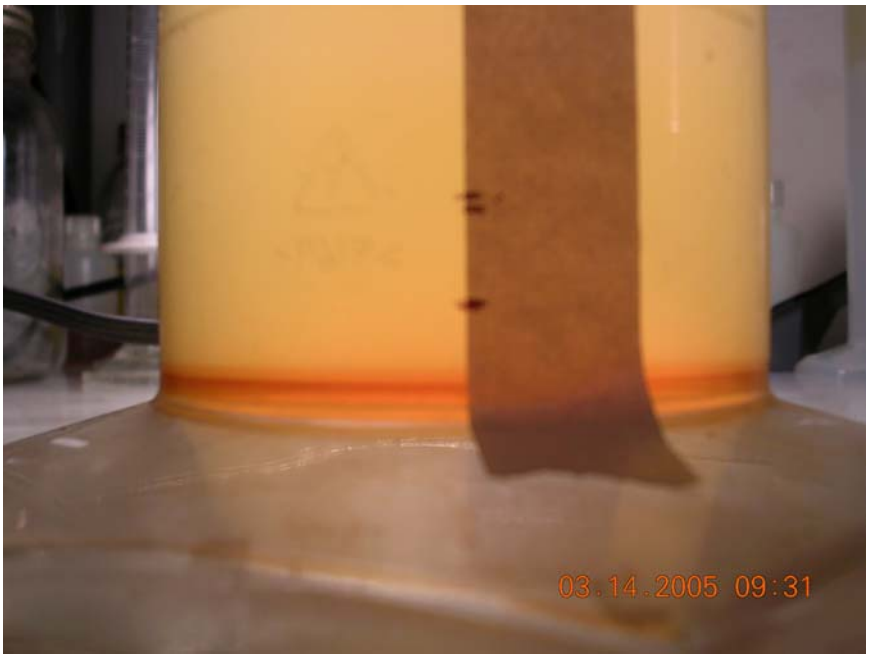

Figure 3.4.1a: Test in progress

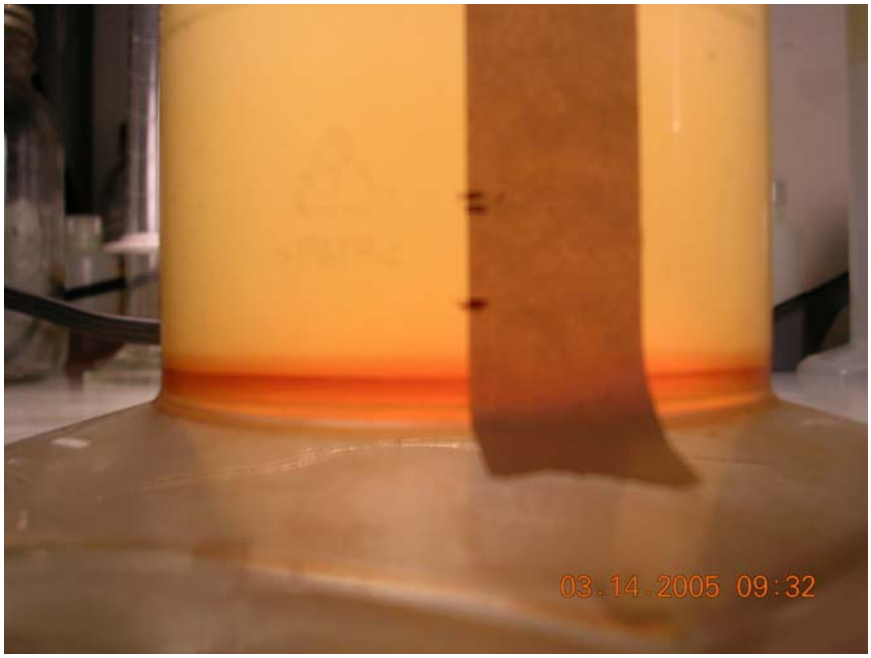

Figure 3.4.1b: Test in progress

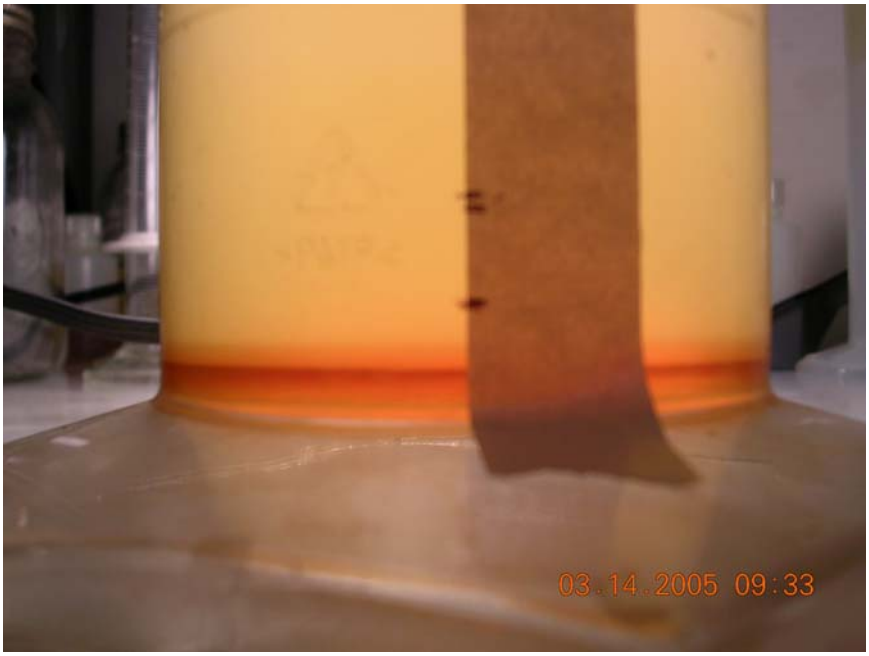

Figure 3.4.1c: Test in progress

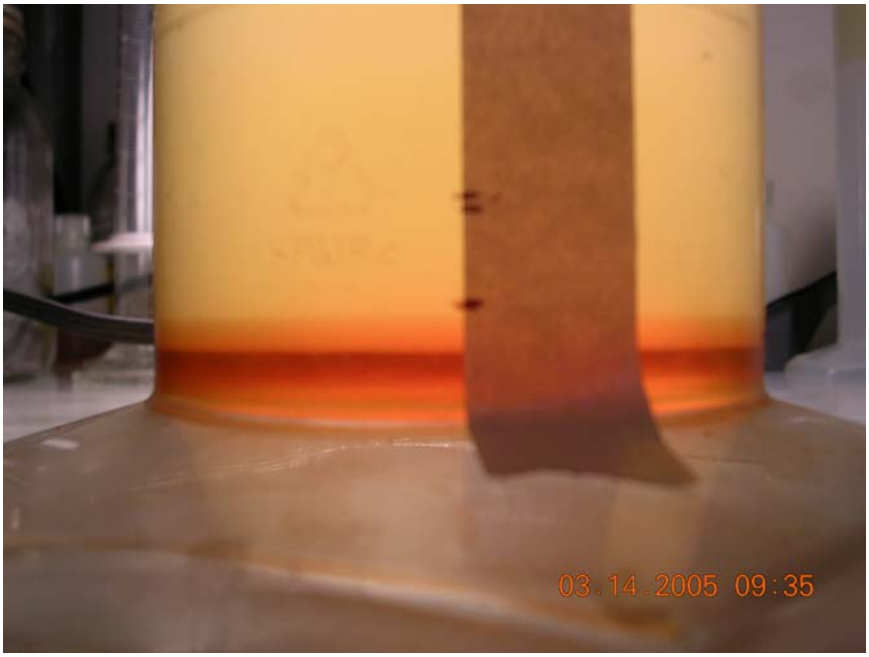

Figure 3.4.1d: Test in progress

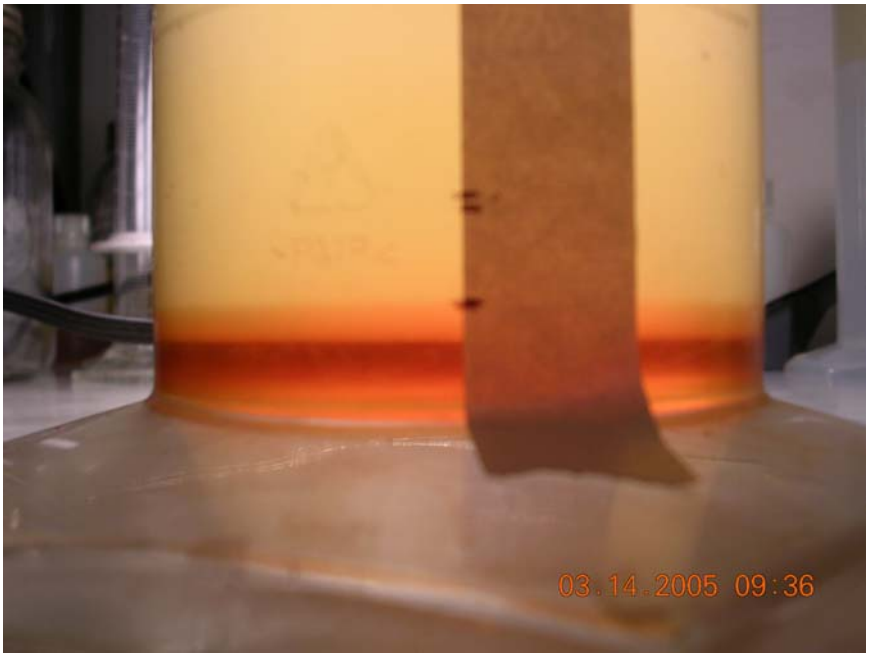

Figure 3.4.1e: Test in progress

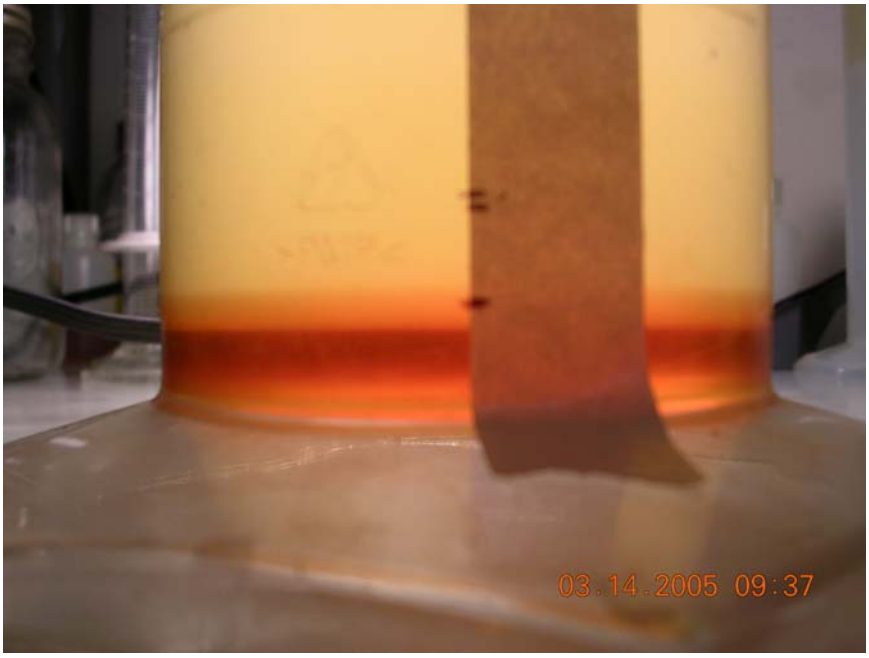

Figure 3.4.1f: Test in progress

Note how the sedimentation front was moving upwards toward the marks on the column. Also note that the liquid-liquid dispersion that was located above the sedimentation front got lighter as time passed due to the fact that the population of the darker glycerin droplets was falling. In these pictures there appears to be a dark band of glycerin sandwiched between two lighter layers; however, this is just an optical illusion caused by the camera. Figure 3.4.2 shows the clear break that is evident at the sedimentation front.

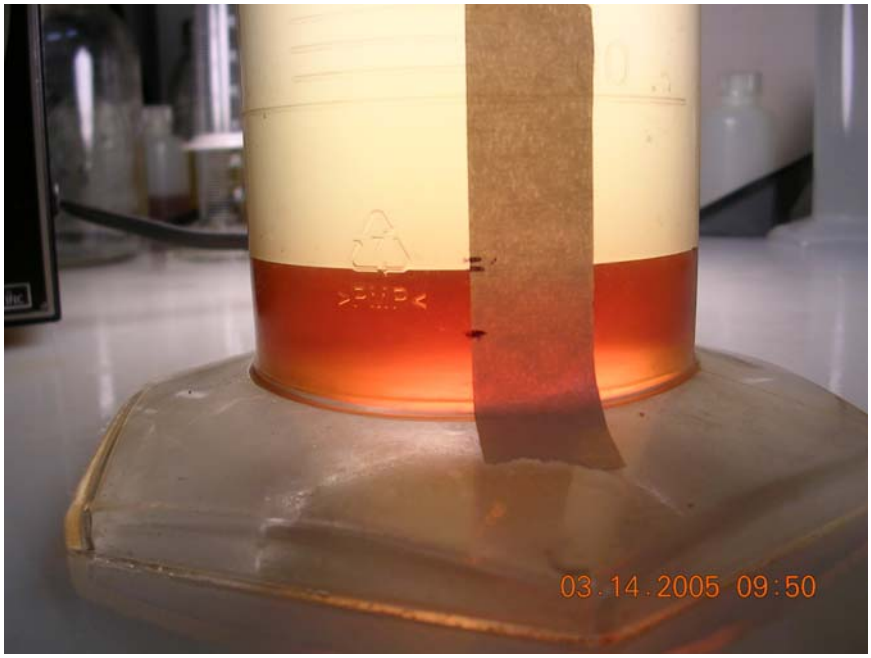

Figure 3.4.2: Fully settled sample

Note in this figure that the sedimentation front has reached the correct level marked on the side of the column; therefore, it is considered fully separated. Also note that the biodiesel is much lighter than the liquid-liquid dispersions in Figures 3.4.1a through 3.4.1f.

3.5 Experimental Data

This section summarizes the experimental data that was recorded for all the tests that were conducted.

A summary of all 20 tests performed for each test setup is provided below.

Table 3.5.1: Experimental data summary

Run #	Time (min)			
	Setup I	Setup II	Setup III	Setup IV
1	21	27	20	22
2	21	26	19	24
3	20	23	21	23
4	19	24	19	23
5	20	27	18	25
6	20	26	20	24
7	18	25	22	26
8	20	25	21	23
9	21	27	18	24
10	19	28	19	25
11	18	26	21	23
12	18	25	20	21
13	20	24	19	22
14	19	26	22	24
15	20	28	21	22
16	18	24	20	21
17	19	25	21	23
18	21	27	22	25
19	19	28	18	24
20	22	26	20	22

In order to better comprehend these times, it is useful to view the data in histogram form. Figures 3.5.1 through 3.5.4 show the number of occurrences of each settling time for each test setup.

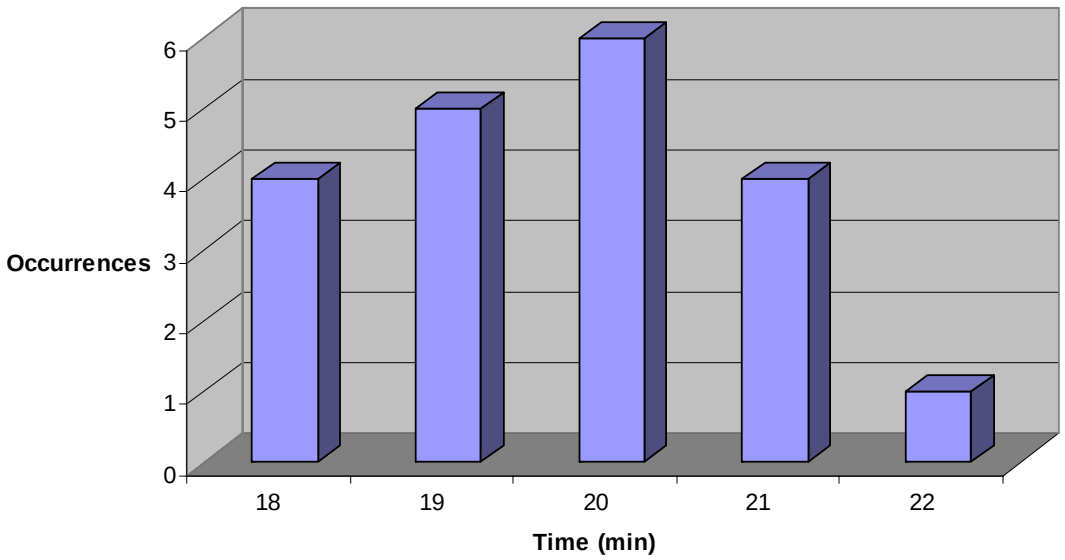

Figure 3.5.1: Histogram for test setup I

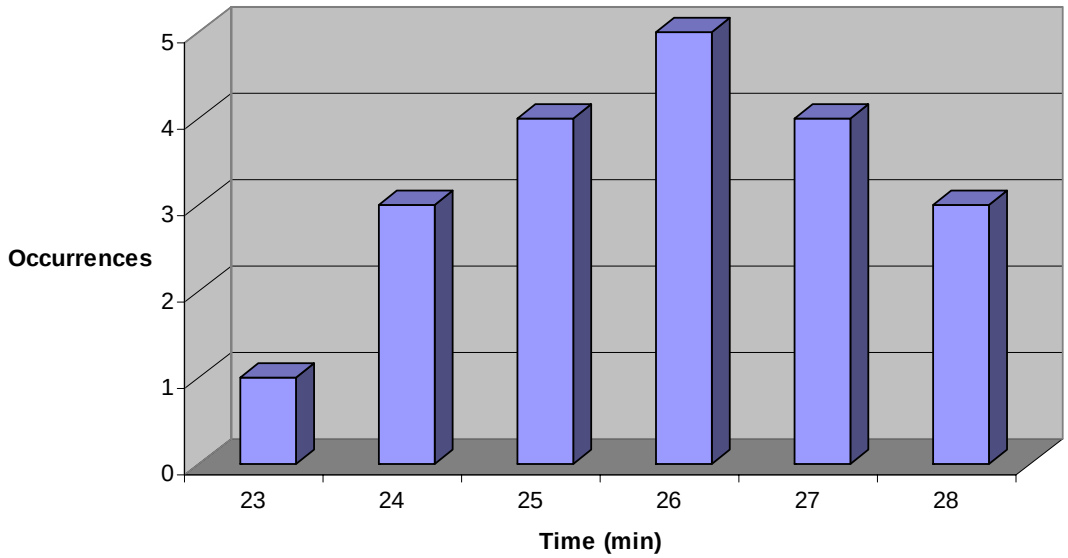

Figure 3.5.2: Histogram for test setup II

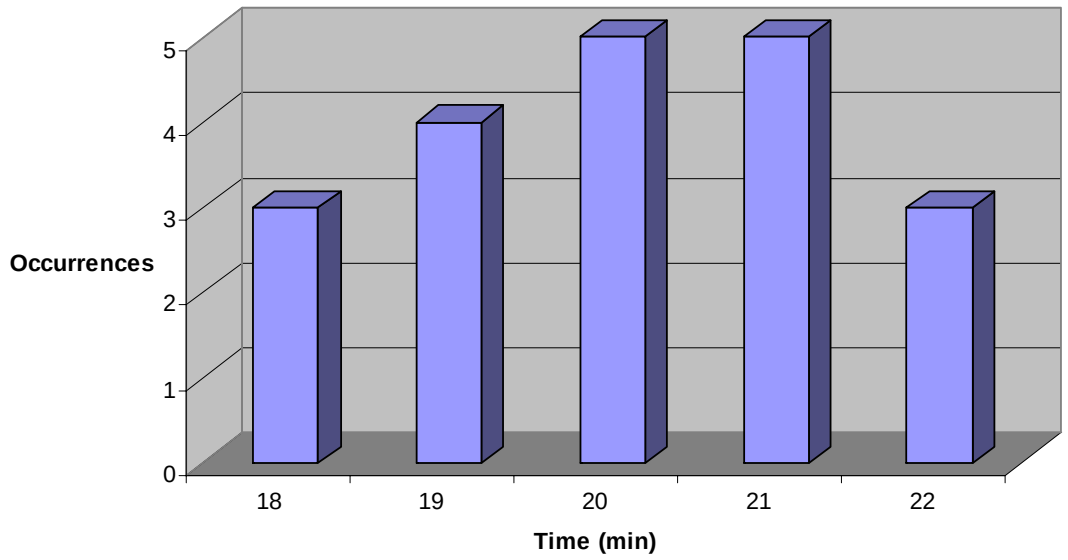

Figure 3.5.3: Histogram for test setup III

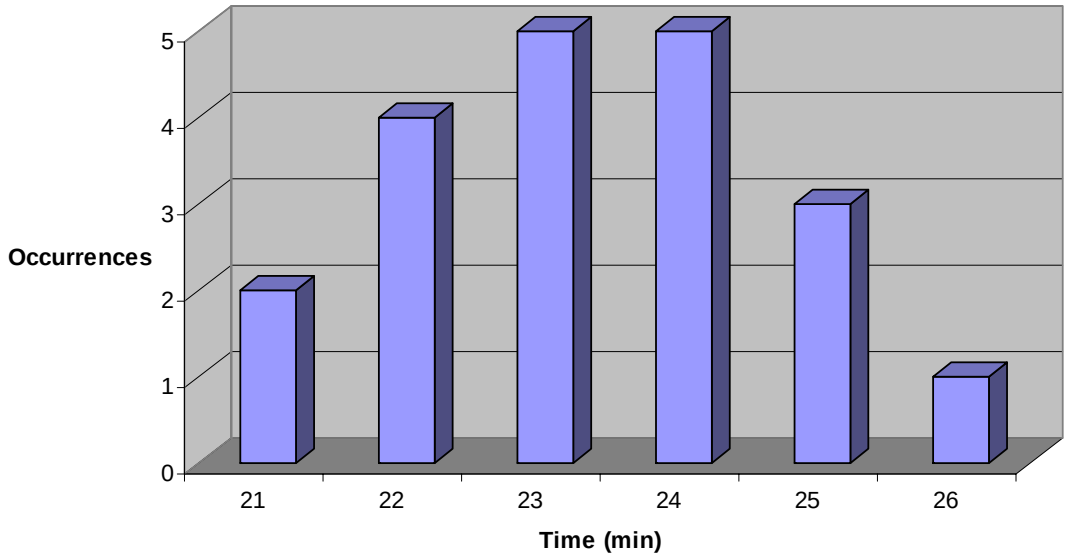

Figure 3.5.4: Histogram for test setup IV

There are no major outlying data points in any of the data presented above. For the most part, the histograms show a slightly bell shaped distribution. This type of distributions indicates that the data is uniformly deviating about a mean value; therefore, the average

settling times should adequately represent the experimental results. These average settling times ranged from 19.7 minutes to 25.9 minutes.

Table 3.5.2: Average settling times

Time (min)			
Setup I	Setup II	Setup III	Setup IV
19.7	25.9	20.1	23.3

One experimental parameter that must also be measured is the initial dispersed phase volume fraction ε_0. After each set of test, the volumes of biodiesel and glycerin were measured. These measurements were then used to determine this volume fraction via (3.2.7).

Table 3.5.3: Volume fraction of glycerin

	Volume (ml)			
	Setup I	Setup II	Setup III	Setup IV
Glycerin	19.3	37.7	49.3	95.1
Biodiesel	215.7	422.3	550.7	1064.9
Mixture	235	460	600	1160
ε_0	0.0821	0.0820	0.0822	0.0820

The values for ε_0 are fairly consistent at just above 0.08. This means that slightly more than 8% of the biodiesel and glycerin mixture is glycerin.

During the experimentations, samples A, B, and C had to be combined in order to have a large enough volume to perform all the tests. Table 3.5.4 describes what sample or combinations of samples were used for each test setup and what order the tests were conducted in.

Table 3.5.4: Explanation of sample usage

Test Setup #	Order Performed	Samples Used
I	1st	A
II	2nd	B
III	3rd	B and C
IV	4th	A, B, and C

At the conclusion of all these tests, a known volume of biodiesel and glycerin was taken from the combined sample as well as from control sample D. These samples were weighted in order to determine their density and each sample was then sent to the North Carolina Department of Agriculture and Consumer Science's Motor Fuels Laboratory for viscosity measurements.

Table 3.5.5: Density and viscosity of fluids

Sample	Description	Density (kg/m^3)	Viscosity (kg/m s)
D	Unused Fuel	882	0.00484
D	Unused Glycerin	1090	0.04740
A, B and C	Used Fuel	878	0.00480
A, B and C	Used Glycerin	1088	0.08000

Note that the densities for biodiesel and glycerin are within several percentage points of each other for the control sample and the experimental sample. The same is true for the viscosity of biodiesel; however, the viscosity of the control glycerin was approximately half that of the experimental glycerin.

Table 3.5.6: Average densities and viscosities

	Density (kg/m3)	Viscosity (kg/m s)
Biodiesel	880	4.82E-03
Glycerin	1089	-

The average viscosity for glycerin was left blank. This parameter will be discussed further in when the choices for $\tilde{g}(\varepsilon_0)$ are examined.

Recall that the model posed by Das can be expressed as

$$\frac{D^2 g(\rho_d - \rho_c)t_s}{18\mu_c L} = \frac{1-\varepsilon_0}{\tilde{g}(\varepsilon_0)}$$

Each parameter in this equation has been reported in this section, except the droplet diameter D. If the model is capable of predicting the settling time for the biodiesel/glycerin, one would only need to determine what droplet diameter allows the model to match experimental data.

3.6 Model vs. Experimental Data

All parameters for Das's model can be assigned a value with the exception of $\tilde{g}(\varepsilon_0)$. Several previous investigators have reported possible expressions for $\tilde{g}(\varepsilon_0)$. In order to determine which relationship for $\tilde{g}(\varepsilon_0)$ to use, each must be compared to the experimental data. The average values for ε_0 and μ_c will be used; however, since there was a discrepancy in the value of μ_d between the control and experimental samples, each of these values will be investigated. The best way to view these relationships, since droplet diameter is not known, is to plot the settling time derived from the model as a function of droplet size.

Table 3.6.1: Possible relationships for $\widetilde{g}(\varepsilon_0)$

Author	$\widetilde{g}(\varepsilon_0)$
Bernea and Mizrahi	$\frac{1-\varepsilon_0}{1+\varepsilon_0^{\frac{1}{3}}}$
Ishii and Zuber	$(1-\varepsilon_0)\frac{\mu_c}{\mu_d}$
Ugarcic	$-0.378\ln(\frac{\varepsilon_0}{1.243})$
Kumar and Hartland	$\frac{1-\varepsilon_0}{1+4.56\varepsilon_0^{0.73}}$

The average settling velocity for the 25.2 cm tests was lower in the 8 cm column (Setup IV) than for the 4.8 cm column (Setup II). Using the data from the 8 cm diameter tests should provide for better analysis since the effects of the cylinder walls were reduced. All further discussion will deal only with data that pertains to a settling column diameter of 8 cm. Figures 3.6.1 through 3.6.4 show these comparisons.

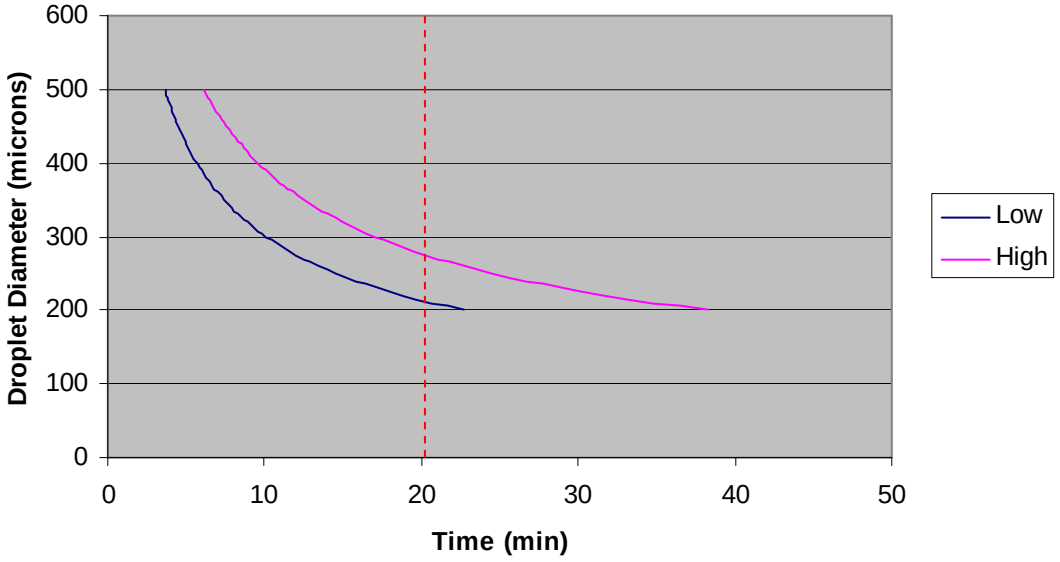

Figure 3.6.1: Ishii model data for L = 13.1 cm

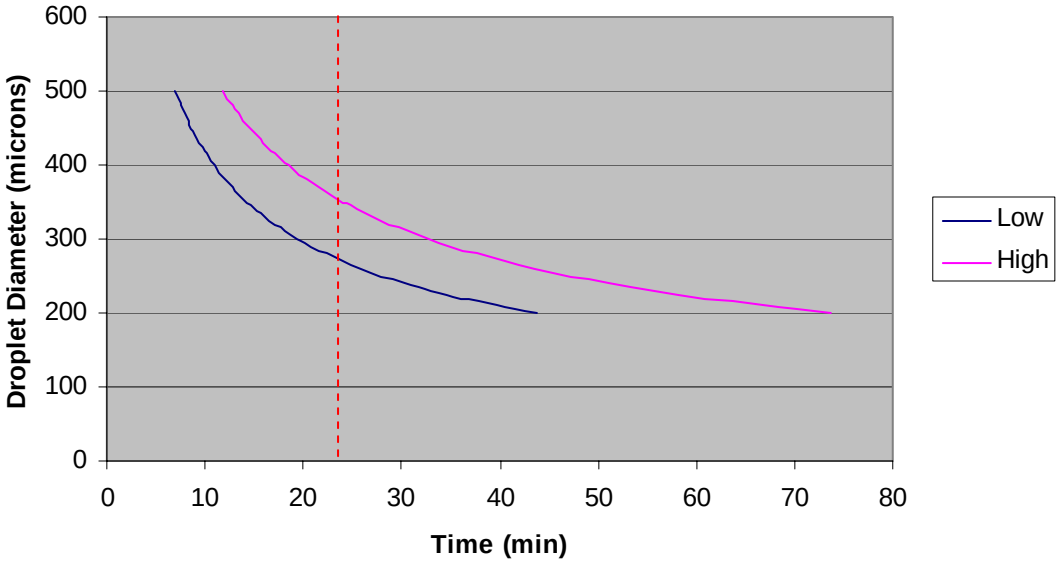

Figure 3.6.2: Ishii model data for L = 25.2 cm

Figures 3.6.1 and 3.6.2 include the model output based on the relationship for $\tilde{g}(\varepsilon_0)$ that was proposed by Ishii. Recall that this relationship used the viscosity of the dispersed phase as an input as well. In these figures, both the low and high values of this viscosity

were used to create the model output for both the 13.1 cm and 25.2 cm column. The red lines on the figures indicate the average experimental settling times of 20.1 minutes and 23.3 minutes for the 13.1 cm and the 25.2 cm column respectively.

The droplet diameters that were needed to force the model to match the experimental data were calculated.

Table 3.6.2: Droplet diameters needed for model output to match experimental data

L (cm)	Droplet Diameter (microns)		
	Low μ_d	High μ_d	Average
13.1	210	275	279
25.2	275	355	

These droplet diameters for each height were averaged to calculate an overall average droplet diameter of 279 microns.

This micron size made it impossible to view the other three relations on the same plots as the Ishii relation. Figures 3.6.3 and 3.6.4 show the other three relationships.

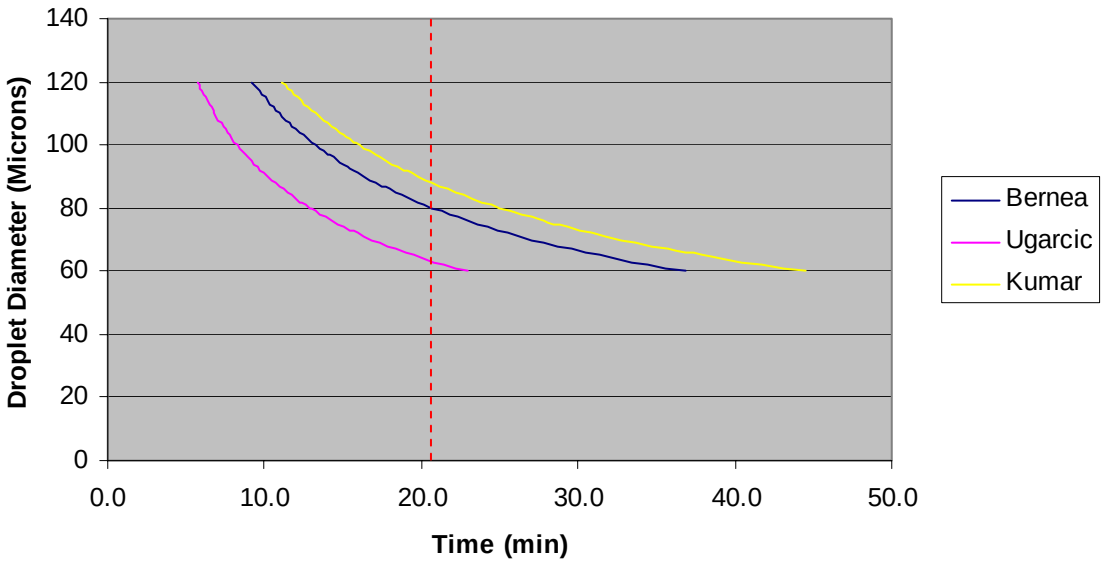

Figure 3.6.3: Model data for L = 13.1 cm

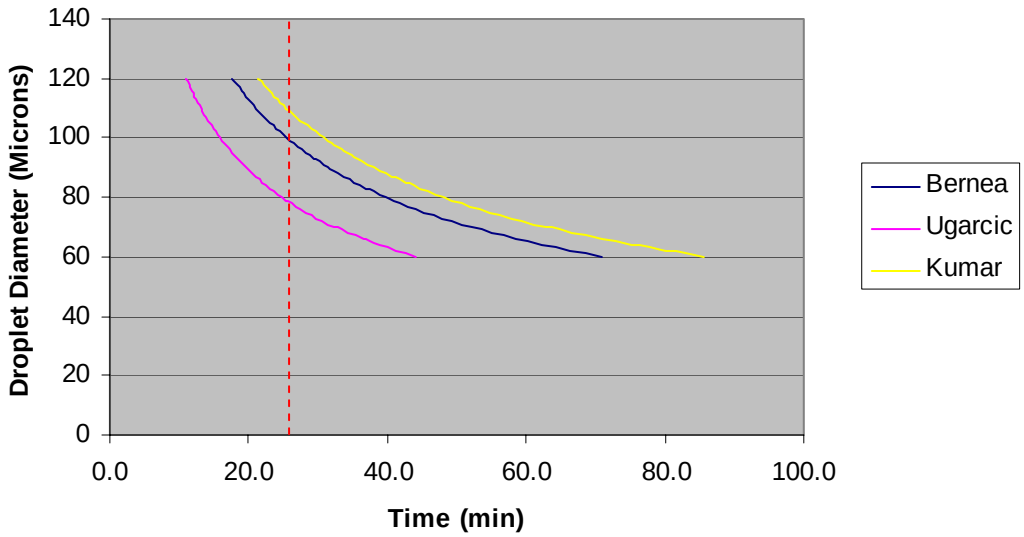

Figure 3.6.4: Model data for L = 25.2 cm

Again, the average experimental settling times are denoted by the vertical red line on each figure. The droplet diameters needed for each relationship to match the experimental data were calculated.

Table 3.6.3: Droplet diameters needed for model output to match experimental data

L (cm)	Droplet Diameter (microns)		
	Bernea	Ugarcic	Kumar
13.1	81	64	89
25.2	105	83	115

The average for each relationship was also calculated, resulting in 93 microns for Bernea, 74 microns for Ugarcic, and 102 microns for Kumar.

Using the average droplet diameters determined for each of the four relationships for $\tilde{g}(\varepsilon_0)$, percent errors were calculated for each column length and then the overall percent error was calculated.

Table 3.6.4: Percent errors for each relationship

Author	L (cm)	Model Time (min)	Experimental Time (min)	Error	Average Error
Ishii	13.1	15.7	20.1	21.9%	26.3%
	25.2	30.2	23.1	30.7%	
Bernea	13.1	15.3	20.1	23.9%	25.8%
	25.2	29.5	23.1	27.7%	
Ugarcic	13.1	15.1	20.1	24.9%	25.2%
	25.2	29	23.1	25.5%	
Kumar	13.1	15.4	20.1	23.4%	25.8%
	25.2	29.6	23.1	28.1%	

For the Ishii relationship, the average dispersed phase viscosity was used in the model to determine these percent errors. The highest percent error was 26.3% for the Ishii relationship, while the lowest percent error of 25.2% belonged to the Ugarcic relationship.

The model proposed by Das doesn't appear to be capable of accurately estimating the settling time of the biodiesel/glycerin mixture. Recall that the model was defined as

$$\frac{D^3 g(\rho_d - \rho_c)t_s}{18\mu_c L} = \frac{1-\varepsilon_0}{\tilde{g}(\varepsilon_0)}$$

where $\tilde{g}(\varepsilon_0)$ can be chosen from one of the four relationships described above.

The values that were used in the final prediction of the errors are presented below.

Table 3.6.5: Parameter summary

Variable	Value	Units
D	7.30E-05	m
g	9.81	m/s2
ρ_d	1089	kg/m3
ρ_c	880	kg/m3
μ_c	4.82E-03	kg/ms
μ_d	6.37E-02	kg/ms
L	0.131 and 0.252	m
ε_0	0.082	-

3.7 Sources of Error

When the model is examined further, it can be seen that settling time scales directly with column height. If the column height is double, the model predicts that the settling time will also double. But investigating the experimental data shows that this is not truly the case. In experimentation, the height was increased by a factor of 1.92, but the settling time only increased by a factor of 1.15. There is no explanation given by Das as to the possible sources of this error. The discrepancies between the models and the experiment were on the order of 25%.

There are several possible causes of these errors in the derivation of the Stokes' Velocity. Recall that it was assumed that the Reynolds number had a value much less than one. Recalling that

$$\mathrm{Re} = \frac{u\rho_c D}{\mu_c}$$

and substituting

$$u = \frac{D^2 g(\rho_d - \rho_c)}{18\mu_c}$$

from Stokes' Law yields

$$\mathrm{Re} = \frac{\rho_c D^3 g(\rho_d - \rho_c)}{18\mu_c^2}$$

Substituting values from Table 3.6.5 into the above equation yields a Reynolds Number range that is well below unity for all the droplet diameters that were considered.

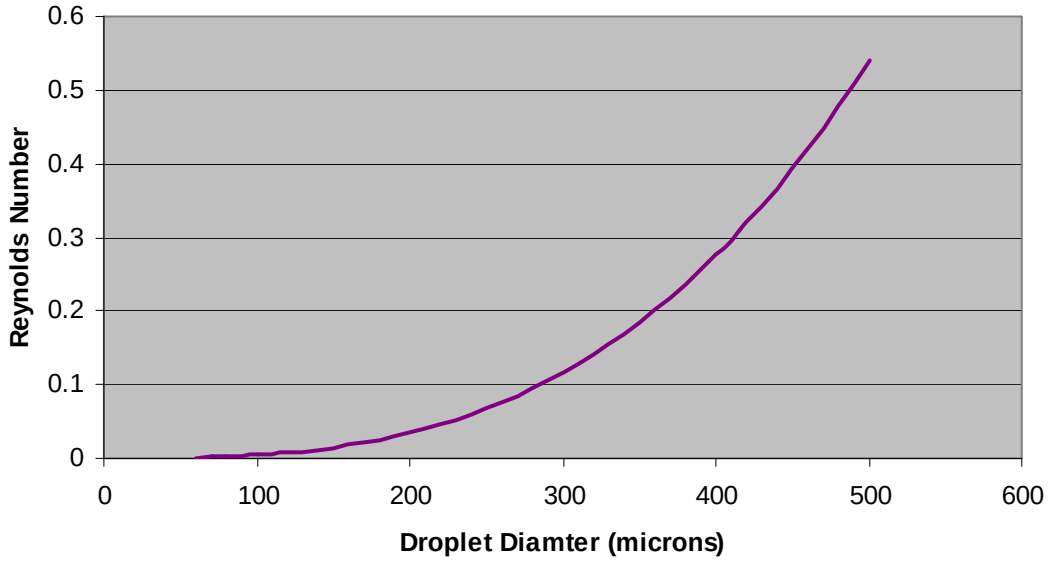

Figure 3.7.1: Reynolds number as a function of droplet size

It was also assumed that the droplets were all of the same size and shape; however, it would be safe to assume that this is not true. There were no testing procedures available that could measure the droplet shape or size; therefore, the impact on this assumption on the

overall error cannot be determined. Das suggests that if this data were available, that the "average diameter… of different size drops can be used without much loss in generality" of the model. Since droplet diameter was chosen to fit the experimental data, if there were different diameters present, then the diameter chosen should have actually been this average diameter.

One would suggest that some error could arise from the viscosities used, especially since the two glycerin viscosities between the control and experimental samples were so different. This discrepancy in viscosity is probably due to the fact that excess alcohol escaped from the samples during experimentation. Upon closer review of the model and the relationships for $\tilde{g}(\varepsilon_0)$, the viscosity of the dispersed phase is not needed to perform any calculations, except for the Ishii relationship; however, this might help explain why this relationship had the largest percent error.

Another possible cause of error was temperature; however, steps were taken to reduce its effects. If the temperature of the liquid-liquid dispersion was different from the ambient temperatures during experimentation, heat transfer and thermal buoyancy forces could have altered the test results. To prevent this from happening, the samples were kept at a room temperature of 20 degrees Celsius at all times and all experiments were carried out at this temperature.

At the onset of this experimentation, when batches of biodiesel and glycerin were first produced (i.e. several minutes after the oil, alcohol, and catalyst were first mixed), coalescing and sedimentation fronts were both observed. However, after allowing the sample to react for several days and agitating the mixture every 24 hours, coalescence was never observed

again. It was hoped that all chemical reactions were complete, in the hopes that any influence from chemical kinetics could be ignored.

One might also argue that coalescence might still be occurring, but it might not be visible and since Das's model is based on a non-coalescing sedimentation process, the model might be inappropriate. To this, Das argues that sedimentation and coalescing are independent functions; therefore, the only consideration that must be made is for the change in droplet size that occurs during coalescing. Here again, since the droplet diameter was chosen to fit the data, this should not be an issue.

Perhaps the most unquantifiable source of error was the human eye. In order to determine the experimental settling time, the sedimentation front was compared against a predetermined height. Utmost care was taken to ensure that the time was recorded as close as possible to the actual moment of settling; however, it is impossible to rule out the fact that errors as much as a minute might have occurred. However, these sources of error were probably not large enough to account for the discrepancies between the models and the experiment.

Recall that the droplet size is squared in the formula for the Stokes' Velocity. Any change in this droplet diameter could greatly affect the output of the model. The smallest predicted droplet size was 64 microns from the Ugarcic relation and the largest diameter of 279 microns resulted from the Ishii relation. Droplet diameters of this size should have produced at least some visible droplets; however, during the duration of the tests, no distinct droplets were ever seen. Instead of droplets falling through the biodiesel, there appears to be a fog of glycerin. Perhaps there were no droplets, especially of visible size, forming in the mixture. This would mean that the Stokes' Velocity is not applicable to this problem;

however, all the literature that was reviewed that dealt with liquid-liquid- separation were based on the Stokes' Velocity. Neither Das nor any other research suggested another form of the settling velocity.

It is believed that glycerin is still dispersed within the biodiesel above the separation front due to the cloudiness of the liquid. If the dispersion is allowed to separate for an extended period of time, for example 24 hours, the biodiesel is almost crystal clear. However, if the mixture is only allowed to settle for 20 minutes or even several hours, there is a noticeable difference in the biodiesel's clarity. It is believed that glycerin is still dispersed within the biodiesel, even after the separation front passes, perhaps as a stable emulsion. If this is true, it directly contradicts the models main assumption that the separation front distinctly separates the continuous phase fluid from the mixture.

During the experimentation the height of the desperation front was used to determine if the mixture was completely settled. The fraction of glycerin that is left dispersed after the separation front has passed was very small; therefore, the height of the separation front appeared to be at its maximum level, even if the mixture was not completely separated. One might suggest that the model is accurately predicting the settling time, but the experimental data is flawed; however, it is known that the biodiesel will not return to its maximum clarity until many hours have passed.

Some of these anomalies could be attributed to the fact that the mixture doesn't consist of pure biodiesel and glycerin. There are small quantities of methanol, catalyst, unreacted tri-, di-, and mono-gylcerides in the mixture. These substances will always be present, for they are a by-product of biodiesel production.

Certainly some of these sources contribute to the overall error, but no one glaring problem can be blamed for the model's shortcomings in this liquid-liquid system. Better measurement of the type of dispersion present and the degree of settling would be valuable additions to further research.

4.1 Production Facility

This research was undertaken to help investigate the possibility of using gravity separation in a continuous production process. The following discussion is based on the assumption that Das's model appropriately estimates the separation time for the biodiesel/glycerin mixture using the Ugarcic relation, since it had the smallest percent error. It is known that Das's model didn't match the empirical data very well; therefore, this discussion should only be used as a guideline. Once empirical data for the biodiesel/glycerin mixture has been collected at the heights and diameters that will be used, the steps described below can be used to accurately design a system.

A continuous production biodiesel facility that was proposed by Peterson and his team from the University of Idaho shows great promise of being implemented in North Carolina.

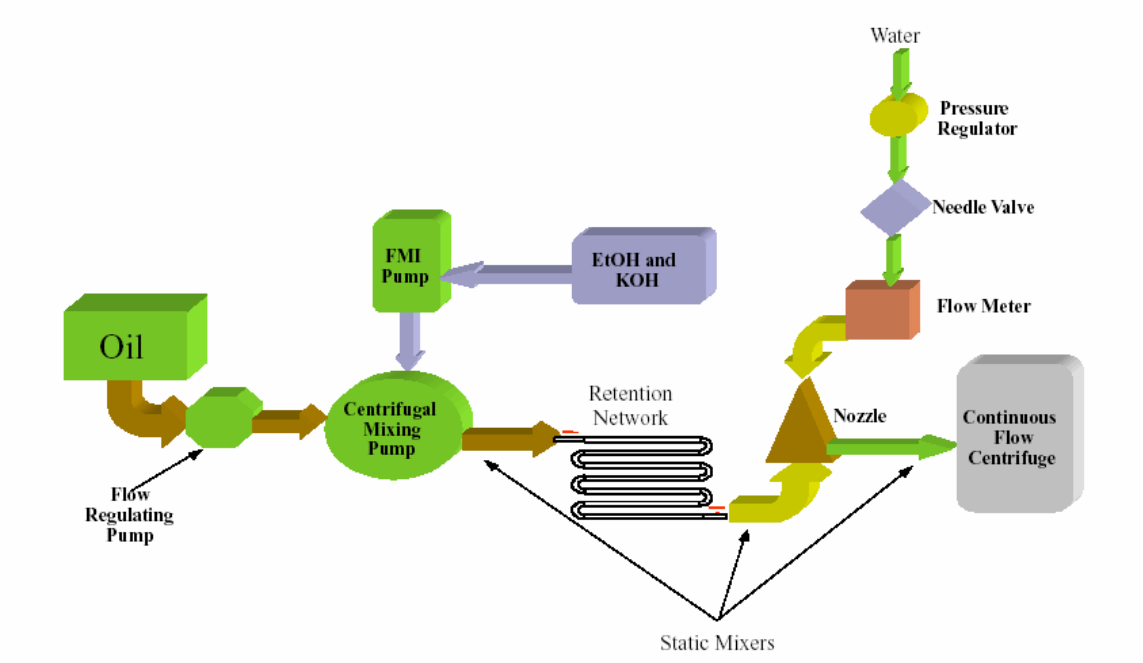

Figure 4.1.1: PFD for Peterson's design (Peterson et al 2002)

This system consists of a centrifugal pump that serves as a mixing pump for the oil, alcohol, and catalyst mixture. This mixture is then sent through a network of pipes that serves as a retention network to allow for completion of the transesterification reaction. Once this mixture has been converted to biodiesel and glycerin, it is fed into a centrifuge for separation. As shown in Figure 4.1.1, ethanol is used instead of methanol; therefore, water is added just before separation. However, this system should be more that capable of producing biodiesel using the recipe that was presented earlier because it relies on the same base catalyzed transesterification reaction. It will be assumed that the biodiesel and glycerin that is leaving this system would be fully reacted.

4.2 Separator Design

This system is capable of producing approximately 500 ml of biodiesel/glycerin per minute; therefore, operating 24 hours a day, 50 weeks a year results in a yearly production of approximately 50,000 gallons of biodiesel per year. This flow rate will be the basis for the separator design. The designed separation system will consist of a collection of cylindrical tanks, whose diameters and heights will be a design choice. The process flow diagram in Figure 4.2.1 will take the place of the centrifuge in Figure 4.1.1. The number of tanks will depend on the time required to settle the mixture based on the height of each tank; however, the diameter of each tank will also affect the number of tanks needed because the more volume per unit height results in fewer tanks needed. The tanks will be sequentially filled with the biodiesel/glycerin mixture. There will be enough storage volume in the tanks to allow enough time for the first tank to separate into two phases and be drained before the last tank is filled. This will ensure that as one tank is filling, one tank will be draining; therefore, there should always be an empty tank ready to accept the biodiesel/glycerin mixture. As the

separated phases leave the bottom of the tank, they will pass through a density sensor that will divert the biodiesel and glycerin into different holding tanks.

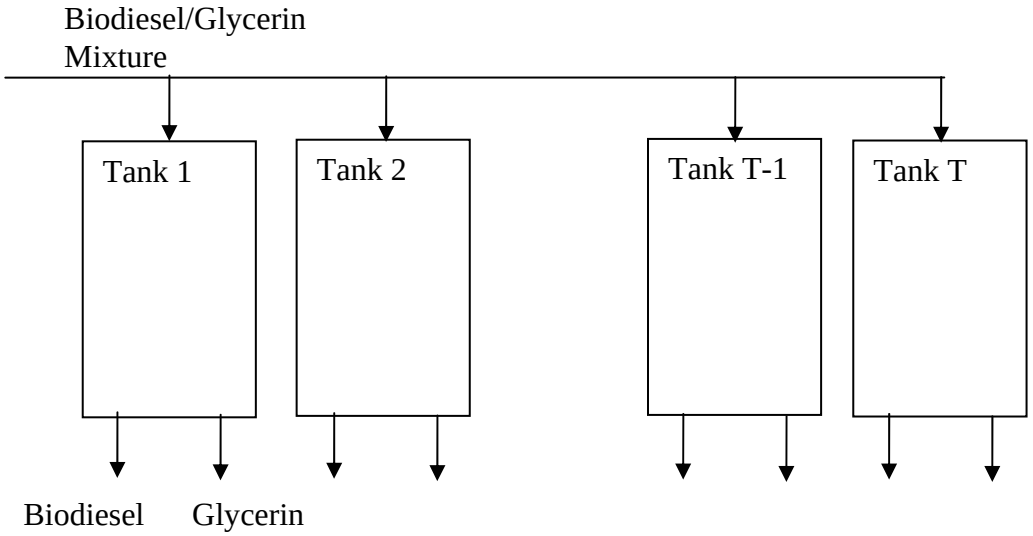

Figure 4.2.1: PFD of designed system

Current biodiesel producers in North Carolina, that are likely to deploy a system such as this, will probably use standard size PVC pipe as much as possible. For this reason, the diameter of the settling tanks was chosen to coincide with standard diameters of PVC pipe. The use of PVC pipe as tanks will allow producers to customize the tank diameter and height easily for their individual needs.

A pipe diameter of six inches was chosen due to the fact that that size of pipe is fairly easy to obtain, yet small enough to work with easily. All the parameters that are described in Table 3.6.5 were entered into the model based on the Ugarcic relation along with a tank diameter of 6 inches.

The last design decision to make is the height of the settling tank; however, since the tank height scales linearly with the settling time, the choice of height was arbitrary. If a taller

tank is chosen, then the volume of the tank will increase as well. This increase in volume results in an increase in the time required to fill the tank and subsequently the time to drain the tank, so the choice of tank height has no effect on the number of tanks needed once all other parameters have been set.

With a known flow rate of 500 ml/min, one can divide the volume of one tank by this flow rate to determine the amount of time necessary to fill the tank. In order to determine the number of tanks needed, the time needed to fill the tank was divided into the time needed to settle the tank. Rounding this number up to the nearest whole number gave the number of tanks needed; however, this number doesn't account for any time to drain the tank. It was assumed that the same amount of time would be necessary to drain the tank as to fill the tank. This assumption forces the use of one additional tank.

A tank height of 24 inches was chosen due to the fact that it provided sufficient time for tank drainage, slightly over 22 minutes. This height results in an estimated separation time of just over 72 minutes. Dividing 72 by 22 and adding 1 determines the number of tanks needed to be 5.

The model overestimated the settling time of the 25.2 cm column; therefore, it is assumed that the model will overestimate the settling times for all column heights above 25.2 cm. If this assumption holds true, then the design described above is over engineered for this application; therefore, it should easily handle the throughput of biodiesel and glycerin that it is designed for.

5 Conclusions

The numerical model that was posed by Das, to predict the settling time of a liquid-liquid dispersion was investigated to determine if it could be used to accurately predict the settling time for a biodiesel/glycerin mixture. Experimentation was conducted to determine the actual settling time required for four different test setups. This experimental time was compared against the time that the model predicted. It was determined that the model was unable to predict the settling time for this mixture over a range of settling conditions with any degree of accuracy. Possible sources for these discrepancies were investigated; however, no one source was determined to be the major contributing factor.

Although the model had percent errors as high as 26.3%, a continuous separation process was designed to mate onto a continuous flow production facility that was developed by researcher at the University of Idaho. A simple bank of 5 small tanks was designed based on Das's model. It was believed that Das's model was vastly overestimating the settling time; therefore, using it to perform a design would mean that the system would be over engineered.

In order to determine if Das's model is capable of modeling production scale facilities, larger scale experimentation must be conducted in the future. This experimentation should included measurement methods to determine the shape, size, and distribution of the glycerin droplets in order to rule out these factors as possible sources of error in the model. Perhaps the most important aspect that this future research should investigate is the height and diameter of the settling columns. Pilot scale, as opposed to laboratory scale, heights and diameters need to be investigated so that scale up to a production scale design would be possible.

6 References

ACS Industries, LP. (2003). *Liquid-liquid coalescer design manual.* Retrieved Feb. 2005, from http://www.acsseparations.com/coalescer_design.htm

Cengel, Y. A., & Boles, M. A. (2002). *Thermodynamics: An engineering approach.* New York, NY: NcGraw-Hill.

Das, P. (1997). Prediction of settling velocity of drops in a concentrated batch liquid-liquid dispersion. *Chemical Engineering and Technology, 20*, 475-477.

Dieter, G. E. (2000). *Engineering design.* New York, NY: McGraw-Hill.

Energy Information Administration. (2005). *Annual energy review.* Retrieved Feb. 2005, from http://www.eia.doe.gov/emeu/aer/petro.html

Frontline. (2002). *Charting the world's oil.* Retrieved Dec. 2004, from http://www.pbs.org/frontlineworld/stories/colombia/oila.html

Holman, J. P. (2001). *Experimental methods for engineers.* New York. NY: McGraw-Hill.

Letterman, R. D. (1999). *Water quality and treatment.* New York, NY: McGraw-Hill.

Marks, L. S., Avallone, E. A., & Baumeister, T. (1999). *Marks' standard handbook for mechanical engineers.* New York, NY: McGraw-Hill.

Nadiv, C. & Semiat, R. (1995). Batch settling of liquid-liquid dispersion. *Industrial and Engineering Chemistry Research, 34*, 2427-2435.

National Biodiesel Board. (2004). *Reports database.* Retrieved Dec. 2004, from http://www.biodiesel.org/resources/reportsdatabase/default.asp

Northeast Sustainable Energy Association. (n.d.). *Biodiesel experiment.* Retrieved Feb. 2005, from http://www.nesea.org/transportation/tour/involved/3.2-Biodiesel%20Experiment.pdf

Pahl, G. (2005). *Biodiesel: Growing a new energy economy.* White River Junction, BT: Chelsea Green Publishing Company.

Perry, R. H., & Green, D. W. (1999). *Perry's chemical engineers' handbook.* New York, NY: McGraw-Hill.

Peterson, C. J., Cook, J. L., Thompson, J. C., & Taberski, J. S. (2002). Continuous flow biodiesel production. *Applied Engineering in Agriculture, 18*(1), 5-11.

White, F. M. (2003). *Fluid mechanics.* New York. NY: McGraw-Hill.